

A Compact and Low-Loss MMI Coupler Fabricated With CMOS Technology

Volume 4, Number 6, December 2012

Zhen Sheng, Member, IEEE

Zhiqi Wang

Chao Qiu

Le Li

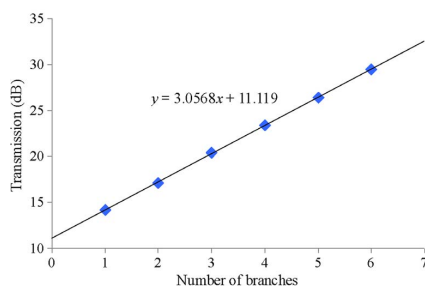
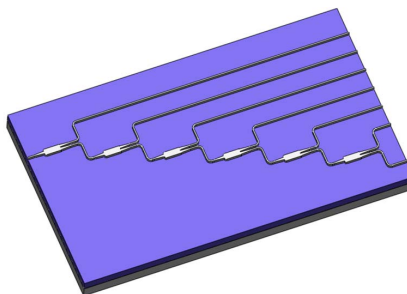
Albert Pang

Aimin Wu

Xi Wang

Shichang Zou

Fuwan Gan



DOI: 10.1109/JPHOT.2012.2230320

1943-0655/\$31.00 ©2012 IEEE

A Compact and Low-Loss MMI Coupler Fabricated With CMOS Technology

Zhen Sheng,¹ *Member, IEEE*, Zhiqi Wang,¹ Chao Qiu,^{1,2} Le Li,² Albert Pang,²
Aimin Wu,¹ Xi Wang,¹ Shichang Zou,^{1,2} and Fuwan Gan¹

¹State Key Laboratory of Functional Materials for Informatics, Shanghai Institute of Microsystem and Information Technology, Chinese Academy of Sciences, Shanghai 200050, China

²Grace Semiconductor Manufacturing Corporation, Shanghai 201203, China

DOI: 10.1109/JPHOT.2012.2230320
1943-0655/\$31.00 ©2012 IEEE

Manuscript received October 23, 2012; revised November 20, 2012; accepted November 21, 2012. Date of publication November 29, 2012; date of current version December 10, 2012. This work was supported in part by the Science and Technology Commission of Shanghai Municipality under Grants 10DJ1400400 and 10706200500, by the Natural Science Foundation of Shanghai under Grant 11ZR1443700, and by the Natural Science Foundation of China under Grants 61106051, 61107031, and 61275112. Corresponding author: Z. Sheng (e-mail: zsheng@mail.sim.ac.cn).

Abstract: We present the design, fabrication, and measurement of a compact and low-loss multimode interference (MMI) coupler based on the silicon nanowire waveguide. The device is carefully designed to achieve both a good performance and a compact size by using the mode matching method. The device is fabricated on silicon-on-insulator (SOI) with 0.13- μm CMOS technology. By measuring the MMI coupler with a cascaded configuration, a very low excess loss of 0.06 dB at the wavelength of 1550 nm is obtained. The device can also work well for a wide wavelength band. The present MMI coupler is very compact with a footprint of $\sim 3.6 \times 11.5 \mu\text{m}^2$ for the multimode region.

Index Terms: Multimode interference (MMI) coupler, low loss, silicon photonics.

1. Introduction

Silicon-on-insulator (SOI) has been considered as a promising platform for photonic integrated circuits (PICs), largely because of its potential process compatibility with CMOS electronics [1]. Besides, the high index contrast between Si and SiO₂ enables it to construct waveguides (usually called photonic wire waveguides, silicon nanowire waveguides, etc.) with submicron cross sections and very small bending radii [2], [3], leading to an ultra-high integration density of photonic devices. Low-loss silicon nanowire waveguides have been demonstrated [4]–[6]. For many applications, optical splitters are frequently used for signal distribution or to construct more complex devices, e.g., Mach–Zehnder interferometers (MZI) [7]. Compared with other kinds of splitters, such as Y-branches [8] and directional couplers [9], multimode interference (MMI) couplers [10] are superior in terms of relaxed fabrication requirements and have been widely used.

Several work has been done to develop high-performance MMI couplers based on the silicon nanowire waveguide. Tsuchizawa *et al.* developed a very compact MMI coupler ($\sim 1.8 \times 2.6 \mu\text{m}^2$) with an excess loss of ~ 0.4 dB [11]. Thomson *et al.* demonstrated an MMI coupler for MZI modulators with an excess loss < 1 dB and a good channel balance [12]. By employing a double etching scheme, the loss of the MMI coupler was reduced to 0.2 dB [13]. In this paper, a compact and low-loss MMI coupler based on silicon nanowire waveguides is realized on SOI with CMOS technology. The device is carefully designed by optimizing various structure parameters. The footprint of the optimal MMI coupler is only $\sim 3.6 \times 11.5 \mu\text{m}^2$ for the multimode region. Through elaborate design

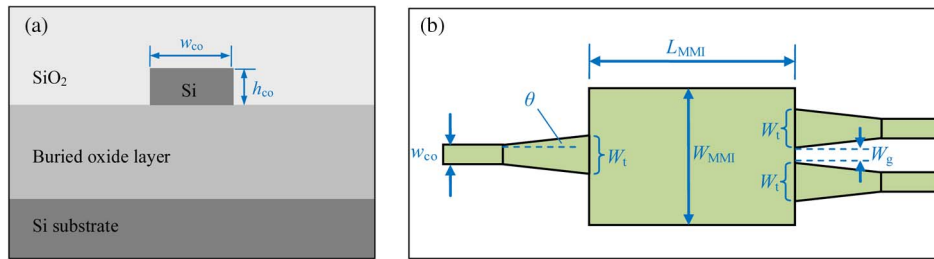


Fig. 1. (a) The cross section of the silicon nanowire waveguide; (b) the schematic of the MMI coupler.

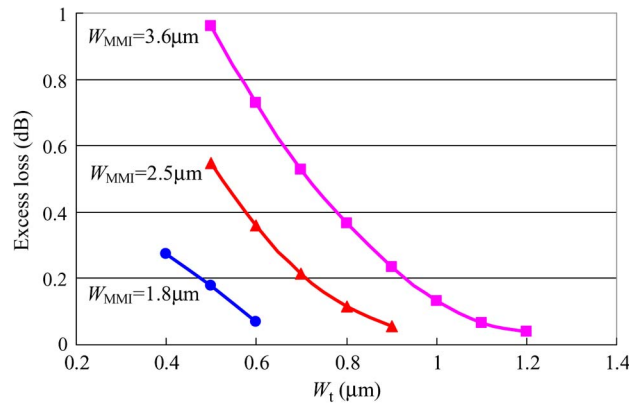


Fig. 2. Simulated excess loss of the MMI coupler with different structure parameters.

and well-controlled fabrication process, the device achieves a very low excess loss of 0.06 dB and a broad operation bandwidth.

2. Design and Fabrication

The MMI coupler considered here is based on the silicon channel waveguide with a width (w_{co}) of 500 nm (for the input and output waveguides) and a height (h_{co}) of 220 nm. Fig. 1(a) and (b) shows the cross section of the silicon channel waveguide that we use and the schematic of the 1×2 MMI coupler, respectively. As shown in Fig. 1(b), the input and output waveguides are broadened through linear tapers. This could help reduce the excess loss by alleviating the mode mismatch between the input/output waveguides and the multimode region, which will be shown in the following.

The operation principle of the MMI coupler is based on the so-called self-imaging theory [10]: in a multimode waveguide, the input field can be reproduced in single or multiple images at periodic intervals along the field propagation direction. For a 1×2 MMI coupler, twofold images are needed. To obtain the imaging position, the beam propagation method (BPM) [14] can be used. However, BPM is not accurate enough for a high index contrast system [15]. Instead, we use the commercial software FIMMWAVE, a full-vectorial simulation tool based on the mode matching method, to find the imaging position and evaluate the device performance, such as the excess loss. Fig. 2 shows the simulation results for TE mode at the wavelength of 1550 nm, where different multimode region widths (W_{MMI}) and different taper widths (W_t) are considered. The length of the multimode region (L_{MMI}) is also optimized for each condition, as it scales proportionally to the square of W_{MMI} and is slightly different as W_t varies for a constant W_{MMI} . One sees that the excess loss is effectively reduced by increasing W_t for each W_{MMI} . This is because a better mode matching happens when the width difference of the access waveguide and the multimode waveguide is smaller [16]. In order to present a more comprehensive comparison, Table 1 summarizes the device performances with

TABLE 1
Device performances with different structure parameters

W_{MMI} (μm)	W_t (μm)	W_g (μm)	Excess loss (dB)	ΔEL (dB)
1.8	0.6	0.3	0.069	0.11
2.5	0.9	0.35	0.055	0.061
3.6	1.2	0.6	0.039	0.027

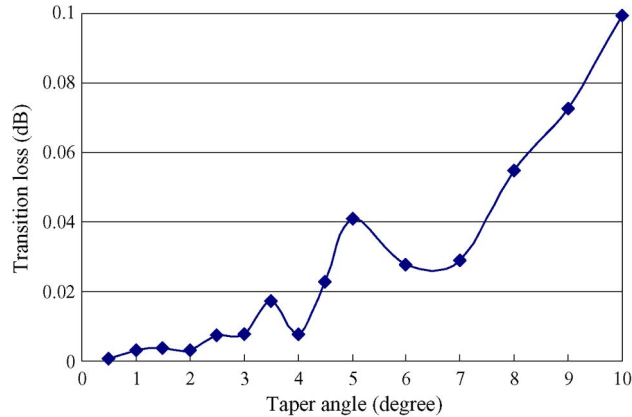


Fig. 3. Transition loss for different taper angles.

different structure parameters, where $W_g (= W_{\text{MMI}}/2 - W_t)$ represents the gap between the two output waveguides [see Fig. 1(b)], and ΔEL is defined as the excess loss degradation when W_t decreases by $0.1\ \mu\text{m}$. Actually, ΔEL is a measure of the fabrication tolerance, i.e., a smaller ΔEL means a larger fabrication tolerance for the device structure parameters. From Table 1, low excess loss ($< 0.1\ \text{dB}$) can be achieved for all the three MMI widths. However, for a smaller MMI width (e.g., $W_{\text{MMI}} = 1.8\ \mu\text{m}$ or $2.5\ \mu\text{m}$), W_g is required to be quite small ($\sim 0.3\ \mu\text{m}$), which is undesirable for the ease of fabrication or for avoiding the intercoupling of the two output waveguides. Moreover, the corresponding ΔEL is quite large, indicating that a precise fabrication process is necessary. Further examination of the excess loss variations with respect to L_{MMI} and W_{MMI} also shows that the device with a larger W_{MMI} has a better fabrication tolerance. As one can imagine, a certain size variation (e.g., $\pm 50\ \text{nm}$) will induce less impact on the device with a larger size than that with a smaller size. Therefore, we choose W_{MMI} and W_t to be $3.6\ \mu\text{m}$ and $1.2\ \mu\text{m}$, respectively, which gives an excess loss of $\sim 0.04\ \text{dB}$. Further increasing W_{MMI} could help improve the device performance further to some extent. However, the device size would become much larger since L_{MMI} scales proportionally to the square of W_{MMI} .

As the input/output waveguides are broadened through linear tapers, the taper length, or more generally, the taper angle θ should be carefully designed to guarantee an adiabatic transition. Fig. 3 shows the transition loss for different taper angles, where the widths of the frontend and backend are fixed as $0.5\ \mu\text{m}$ and $1.2\ \mu\text{m}$, respectively. Generally, the transition loss increases as the taper angle increases. The local minima and maxima in Fig. 3 are induced by the higher order mode excitation when the taper angle is not small enough for an adiabatic transition. The taper loss should be kept much smaller than the intrinsic MMI loss (i.e., $0.04\ \text{dB}$ in this case) as it is only an additional loss induced by auxiliary structures. Therefore, we choose $\theta = 1^\circ$, which corresponds to a taper loss of $0.003\ \text{dB}$ and is negligible compared with the intrinsic MMI loss. It is worth to mention that the taper optimization is necessary since the taper transition loss may even overwhelm the intrinsic MMI loss when the taper is not carefully designed.

The optimal device parameters are summarized as follows: $W_{\text{MMI}} = 3.6\ \mu\text{m}$, $W_t = 1.2\ \mu\text{m}$, $W_g = 0.6\ \mu\text{m}$, $L_{\text{MMI}} = 11.5\ \mu\text{m}$, and $\theta = 1^\circ$.

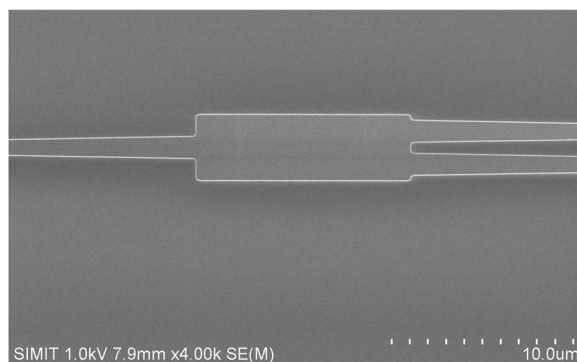


Fig. 4. SEM picture of the fabricated MMI coupler.

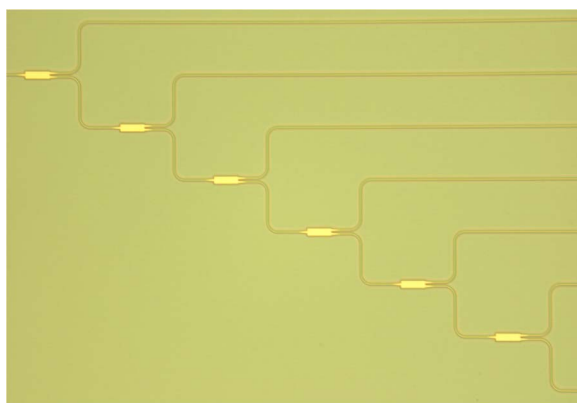


Fig. 5. Microscopic picture of the MMI couplers arranged in a cascaded configuration.

The devices were fabricated on SOI with 0.13- μm CMOS technology. We started from the 200-mm SOI wafer with a top silicon layer of 220 nm and a buried oxide (BOX) layer of 2 μm . A silicon nitride (SiN) film was first deposited on the wafer surface as a hard mask layer for the subsequent Si etching. 248-nm deep-ultraviolet (DUV) lithography was then used to define the waveguide pattern. To reduce the sidewall roughness, the thickness of the bottom anti-reflection coating (BARC) layer and the exposure condition were both optimized. After transferring the photoresist pattern to the SiN hard mask, silicon waveguides were formed using inductively coupled plasma reactive ion etching (ICP-RIE). The silicon etching recipe was tuned to achieve both a smooth sidewall and a vertical profile. Finally, a thick SiO_2 layer was deposited on the wafer surface. The SEM picture of the fabricated MMI coupler is shown in Fig. 4. The footprint of the multimode region is $\sim 3.6 \times 11.5 \mu\text{m}^2$. For efficient fiber coupling, shallow-etched grating couplers [17] for TE mode were fabricated on chip at each input/output end.

3. Measurement and Discussion

The propagation loss of the fabricated waveguides was first measured to be 2.4 dB/cm through the cutback method. To determine the excess loss of the device, we measured the transmission of the MMI couplers arranged in a cascaded configuration, as shown in Fig. 5. Then, the excess loss of the device can be deduced by comparing the transmission after different number of branches. Fig. 6 shows the measured results for TE mode at the wavelength of 1550 nm, where the data is linearly fitted. The equation of the fitted line is also shown. The excess loss can be extracted through the slope of the fitted line and is ~ 0.06 dB. This value is very small and is comparable with the

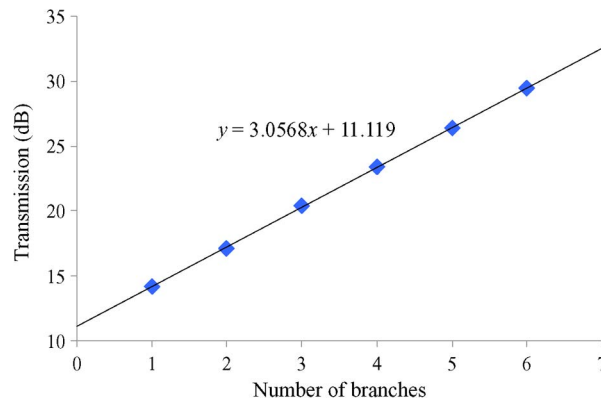


Fig. 6. Measured transmission of the cascaded MMI couplers at the wavelength of 1550 nm.

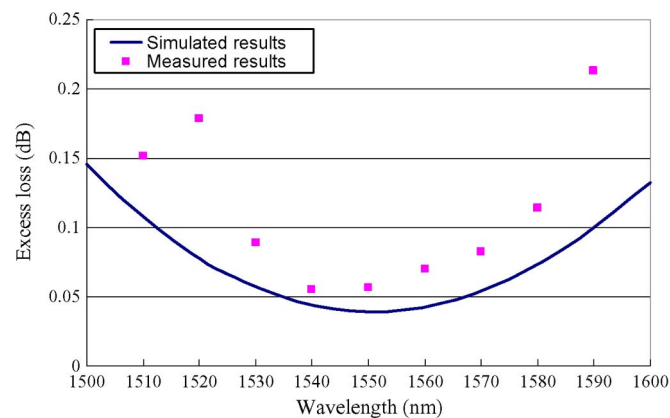


Fig. 7. Simulated and measured excess loss for different wavelengths.

simulated result. The y -intercept (11.1 dB) represents the coupling loss of the two fiber-coupling interfaces, which agrees well with the coupling efficiency of the present shallow-etched grating couplers.

Fig. 7 shows the measured excess loss for different wavelengths. For comparison, the simulated results are also shown. One sees that very low excess loss (< 0.1 dB) is obtained experimentally for the wavelength range of 1530 nm \sim 1570 nm. Note that the measured results for the wavelengths far from the central wavelength of the grating coupler (i.e., ~ 1550 nm) are less reliable since the linearity of the measured data is poorer for those wavelengths. This is because the coupling efficiencies of different grating couplers are a little different for those wavelengths. Nonetheless, the simulated results indicate that the present MMI coupler can work well for a wide wavelength band from 1500 nm to 1600 nm.

4. Conclusion

The design, fabrication, and measurement of a compact and low-loss MMI coupler have been demonstrated. The intrinsic MMI loss is minimized through careful design of the structure parameters. To minimize the transition loss induced by the taper structures, the taper angle is optimized. The device has been fabricated in a $0.13\text{-}\mu\text{m}$ CMOS line with improved DUV lithography and etching processes. The measured excess loss of the fabricated 1×2 MMI coupler is only 0.06 dB as a synthetic result of elaborate design and well-controlled fabrication process. The device can also work well for broadband applications. The high-performance MMI coupler can be used to construct more complex devices, such as MZI modulators.

References

- [1] M. Lipson, "Guiding, modulating, and emitting light on silicon—challenges and opportunities," *J. Lightw. Technol.*, vol. 23, no. 12, pp. 4222–4238, Dec. 2005.
- [2] D. Dai, Y. Shi, and S. He, "Characteristic analysis of nanosilicon rectangular waveguides for planar light-wave circuits of high integration," *Appl. Opt.*, vol. 45, no. 20, pp. 4941–4946, Jul. 2006.
- [3] Z. Sheng, D. Dai, and S. He, "Comparative study of losses in ultrasharp silicon-on-insulator nanowire bends," *IEEE J. Sel. Topics Quantum Electron.*, vol. 15, no. 5, pp. 1406–1412, Sep./Oct. 2009.
- [4] Y. A. Vlasov and S. J. McNab, "Losses in single-mode silicon-on-insulator strip waveguides and bends," *Opt. Exp.*, vol. 12, no. 8, pp. 1622–1631, Apr. 2004.
- [5] T. Tsuchizawa, K. Yamada, H. Fukuda, T. Watanabe, J. Takahashi, M. Takahashi, T. Shoji, E. Tamechika, S. Itabashi, and H. Morita, "Microphotonics devices based on silicon microfabrication technology," *IEEE J. Sel. Topics Quantum Electron.*, vol. 11, no. 1, pp. 232–240, Jan. 2005.
- [6] P. Dumon, W. Bogaerts, V. Wiaux, J. Wouters, S. Beckx, J. Van Campenhout, D. Taillaert, B. Luyssaert, P. Bienstman, D. Van Thourhout, and R. Baets, "Low loss SOI photonic wires and ring resonators fabricated with deep UV lithography," *IEEE Photon. Technol. Lett.*, vol. 16, no. 5, pp. 1328–1330, May 2004.
- [7] F. Ohno, T. Fukazawa, and T. Baba, "Mach–Zehnder interferometers composed of μ -bends and μ -branches in a Si photonic wire waveguide," *Jpn. J. Appl. Phys.*, vol. 44, no. 7A, pp. 5322–5323, Jul. 2005.
- [8] S. H. Tao, Q. Fang, J. F. Song, M. B. Yu, G. Q. Lo, and D. L. Kwong, "Cascade wide-angle Y-junction 1×16 optical power splitter based on silicon wire waveguides on silicon-on-insulator," *Opt. Exp.*, vol. 16, no. 26, pp. 21 456–21 461, Dec. 2008.
- [9] Y. Quan, P. Han, Q. Ran, F. Zeng, L. Gao, and C. Zhao, "A photonic wire-based directional coupler based on SOI," *Opt. Commun.*, vol. 281, no. 11, pp. 3105–3110, Jun. 2008.
- [10] L. Soldano and E. Pennings, "Optical multi-mode interference devices based on self-imaging: Principles and applications," *J. Lightw. Technol.*, vol. 13, no. 4, pp. 615–627, Apr. 1995.
- [11] T. Tsuchizawa, K. Yamada, H. Fukuda, T. Watanabe, S. Uchiyama, and S. Itabashi, "Low-loss Si wire waveguides and their application to thermo optic switches," *Jpn. J. Appl. Phys.*, vol. 45, no. 8B, pp. 6658–6662, Aug. 2006.
- [12] D. J. Thomson, Y. Hu, G. T. Reed, and J.-M. Fedeli, "Low loss MMI couplers for high performance MZI modulators," *IEEE Photon. Technol. Lett.*, vol. 22, no. 20, pp. 1485–1487, Oct. 2010.
- [13] W. Bogaerts, S. K. Selvaraja, P. Dumon, J. Brouckaert, K. De Vos, D. Van Thourhout, and R. Baets, "Silicon-on-insulator spectral filters fabricated with CMOS technology," *IEEE J. Sel. Topics Quantum Electron.*, vol. 16, no. 1, pp. 33–44, Jan. 2010.
- [14] C. B. Ma and E. Van Keuren, "A three-dimensional wide-angle BPM for optical waveguide structures," *Opt. Exp.*, vol. 15, no. 2, pp. 402–407, Jan. 2007.
- [15] Y. Jiao, Y. Shi, D. Dai, and S. He, "Accurate and efficient simulation for silicon-nanowire-based multimode interference couplers with a 3D finite-element mode-propagation analysis," *J. Opt. Soc. Amer. B, Opt. Phys.*, vol. 27, no. 9, pp. 1813–1818, Sep. 2010.
- [16] Y. Shi, D. Dai, and S. He, "Improved performance of a silicon-on-insulator-based multimode interference coupler by using taper structures," *Opt. Commun.*, vol. 253, no. 4–6, pp. 276–282, Sep. 2005.
- [17] D. Taillaert, F. Van Laere, M. Ayre, W. Bogaerts, D. Van Thourhout, P. Bienstman, and R. Baets, "Grating couplers for coupling between optical fibers and nanophotonic waveguides," *Jpn. J. Appl. Phys.*, vol. 45, no. 8A, pp. 6071–6077, Aug. 2006.